Int. J. Electrochem. Sci., 12 **(2017)** 5668 – 5691, doi: 10.20964/2017.06.86

International Journal of ELECTROCHEMICAL SCIENCE
www.electrochemsci.org

Assessment of the Inhibition Efficiency of 3-amino-5-methylthio-1H-1,2,4-triazole Against the Corrosion of Mild Steel in Acid Chloride Solution

Mieczyslaw Scendo[*], *Katarzyna Staszewska-Samson*

Institute of Chemistry, Jan Kochanowski University in Kielce, Swietokrzyska 15G, PL- 25406 Kielce, Poland
[*]E mail: scendo@ujk.edu.pl

Received: 13 March 2017 / *Accepted:* 29 April 2017 / *Published:* 12 May 2017

Influence of 3-amino-5-methylthio-1H-1,2,4-triazole (AMTTA) concentration on the corrosion of C45 mild steel in acid chloride solutions were studied. The potentiodynamic (PD) polarization, electrochemical impedance spectroscopy (EIS) methods and quantum chemical calculations were used. The surface morphology of specimens were observed through inverted metallographic microscope (IMM). It has been shown that the inhibition efficiency increased with an increase in the concentration of 3-amino-5-methylthio-1H-1,2,4-triazole. Tafel polarization study revealed that AMTTA acted as mixed type inhibitor. The best fit to the experimental data was obtained using Temkin adsorption isotherm. It was found that the adsorption of inhibitor on the mild steel surface takes place through a typical physisorption. Moreover, the adsorption mechanism of AMTTA on C45 mild steel surface was proposed and discussed.

Keywords: A. C45 mild steel; A. 3-amino-5-methylthio-1H-1,2,4-triazole; C. Inhibition efficiency; C. Corrosion rate; C. Temkin adsorption isotherm

1. INTRODUCTION

Mild steel (MS) is widely used as a construction material in many industries due to its excellent mechanical properties and low cost. Unfortunately, the main problem of applying of MS is its dissolution in acidic environments [1]. The use of organic compounds to inhibit corrosion of mild steel has assumed great significance due to their application in preventing corrosion under various corrosive environments. The inhibition efficiency of organic compounds are strictly related with its molecular structure which is responsible for the adsorptive interaction strength with the metal surface. Moreover,

inhibition efficiency is highly influenced by the surface conditions and nature of corroding system, as well as the corrosive environment [2,3]. Most of the well-known organic inhibitors are heterocyclic compounds containing π-electrons, heteroatoms like nitrogen, oxygen or sulphur and aromatic rings [4,5]. These molecules are strongly adhered to metal surface and block the active centers, generally forming a protective film. The compounds previously studied as inhibitors of mild steel include: bipyrazolic derivatives [6], surfactants [7], aromatic hydrazides [8], organic dyes [9] and thiosemicarbazide type organic compounds [10]. Many kind of nitrogen containing compounds (as heteroatoms or amine group) have been investigated in variety corrosive environment such as: chloride solution [11,12], carbon dioxide saturated chloride solution [13,14], alkaline chloride solution [15] or cooling water system [16] as an effective corrosion inhibitors. Many substituted triazole compounds have been studied in considerable details as effective corrosion inhibitors for steel [17-23]. In the past few years the inhibition of mild steel corrosion in acid solutions by various of 1,2,4-triazole compounds have attracted more attention. This problem will be considered in detail in the further part of the paper. It is know that the primary step in the action of organic corrosion inhibitors in acid solutions is usually strong adsorption at the metal surface. Furthermore, the adsorption requires the existence of attractive forces between the adsorbate and the substrate surface. The triazole derivatives have special affinity towards metal surface displacing water molecules on the surface. They possess abundant π -electrons and unshared electron pairs on the nitrogen atom that can interact with *d*-orbitals of iron to provide a protective film. Therefore, the stability of the adsorbed inhibitor film on the metal surface depends on some physicochemical properties of the molecule of compounds [24,25].

However, in the available scientific literature are missing research results about the 3-amino-5-methylthio-1H-1,2,4-triazole (AMTTA) as corrosion inhibitor of mild steel, especially in acid chloride solution.

The present work intends to study the corrosion behavior of C45 mild steel in acid chloride solution without or with of 3-amino-5-methylthio-1H-1,2,4-triazole. The inhibition performance of AMTTA was studied by potentiodynamic polarization, electrochemical impedance spectroscopy methods and quantum chemical calculations. The surface of mild steel was observed by inverted metallographic microscope.

2. EXPERIMENTAL

2.1. Reagents

The following reagents were used to make the solutions: of 3-amino-5-methylthio-1H-1,2,4-triazole (AMTTA), sodium chloride, and hydrochloric acid. All chemicals were purchased from Sigma-Aldrich products. The test solutions were prepared from analytical-grade chemical reagents in distilled water (three times) without further purification. The corrosive environment was obtained by mixing the sodium chloride (1 M) and hydrochloric acid (1 M), so the concentration of Cl^- ions were 1.2 M and pH was 1.5. For each experiment a freshly made solutions were used. All test have been performed in naturally aerated electrolytes.

2.2. Electrodes

The working electrode was made from C45 mild steel. The elemental composition of the steel was as follows (wt.%): C: 0.42-0.5; Mn: 0.5-0.8; Si: 0.1-0.4; P: max 0.04; S: max 0.04; Cr: max 0.3; Ni: max 0.3; Mo: max 0.3; Cu: max 0.3; and Fe balance.

For all experiments a standard electrochemical cell with three electrodes was used. All solutions have the same volume of 100 cm^3. The working electrode was prepared in the shape of rectangle which had a surface area of 0.78 cm^2. Prior to each experiment, the working electrode surface was treated with 800, 1200, and 2000 grade emery paper to give a mirror like surface finish, and then thoroughly rinsed with double distilled water. After this the electrode was degreased with ethanol in an ultrasonic bath (about 5 min) and then rinsed with double distilled water. The working electrode immediately after cleaning was immersed in the test electrolyte.

The Ag/AgCl electrode was used as the reference system. It was connected with the solution by a Luggin capillary. The capillary tip was opposite about 3 mm to the end of the surface working electrode.

The counter electrode (with a 5 cm^2 surface area) was made from platinum foil (99.99% Pt).

However, the reference and counter electrodes were individually isolated from the test solution by adjusted accordingly glass frits.

2.3. Measuring instruments

Potentiostat/galvanostat PGSTAT 128N, AutoLab, Netherlands with NOVA 1.7 (software the same firm) was employed for potentiodynamic polarization and electrochemical impedance spectroscopy measurements. The experiments were carried out open to the atmosphere and each measurements were realized with freshly prepared specimens. The values reported in the paper represent mean values of at least three replicate measurements.

Surface topography of the test specimens were observed by inverted metallographic microscope, Delta Optical IM-100.

All experiments were carried out at suitably well-chosen temperature (25±0.5 ^{0}C) which was maintained by a thermostat with the forced air circulation.

2.4. Testing methods

The electrochemical behaviour of C45 mild steel specimen in uninhibited and inhibited solution was studied by recording potentiodynamic polarization curves. The polarization curves were obtained by automatically changing the electrode potential from -800 to 0 mV (vs. Ag/AgCl) at a scan rate of 1 mV s^{-1}.

Polarization studies have been made to generate knowledge concerning the kinetics of cathodic and anodic reactions. The linear Tafel segments of cathodic and anodic curves were extrapolated to corrosion potential (E_{corr}) to obtain corrosion current densities (j_{corr}) and cathodic (β_c) or anodic (β_a) of the Tafel slopes, follow the equation:

$$j = j_{corr}\left\{\exp\left[\frac{2.303(E - E_{corr})}{\beta_a}\right] - \exp\left[\frac{-2.303(E - E_{corr})}{\beta_c}\right]\right\}. \quad (1)$$

The inhibition efficiency was calculated basis on the following equation [26,27]**:**

$$\eta(\%) = \frac{j^0_{corr} - j_{corr}}{j^0_{corr}} \times 100, \quad (2)$$

where j_{corr} and j^0_{corr} are the corrosion current densities in the absence and presence of the inhibitor, respectively in the test solution.

The linear polarization resistance measurements were carried out by recording the electrode potential ±25 mV around corrosion potential (Stern plots). However, the polarization resistance (R_p) was determined according to Stern-Geary equation:

$$j_{corr} = \frac{b_c\, b_a}{2.303(b_c + b_a)}\frac{1}{R_p}, \quad (3)$$

and:

$$B = \frac{b_c\, b_a}{2.303(b_c + b_a)}, \quad (4)$$

where b_a and b_c are the coefficients of the electrode reactions. The coefficients values can be graphically defined as the slope of the straight lines of the polarization curves in the logarithmic current density scale. The polarization resistance can be expressed as:

$$R_p = \frac{B}{j_{corr}}. \quad (5)$$

The corrosion rate were calculated using the formula:

$$v_p = \frac{t\, j_{corr}\, M}{n\, F\rho}. \quad (6)$$

Moreover, mass corrosion rate (destruction corrosive material) was calculated according to the Faraday's equation:

$$\Delta m = \frac{t\, j_{corr}\, M}{n\, F}, \quad (7)$$

where t is the duration time of the corrosion process, M is the molar mass of the metal, n is the number of electrons transferred in the corrosion reaction, F is the Faraday constant, and ρ is the density of the corroded material.

Moreover, the electrochemical impedance spectroscopy (EIS) measurements were realized at corrosion potential (E_{corr}). The employed frequency range was 100 kHz to 0.01 Hz and the amplitude was 10 mV.

2.5. Theoretical details

HyperChem version 7.5 a quantum-mechanical program (Hypercube Inc) was used for molecular modeling of 3-amino-5-methylthio-1H-1,2,4-triazole molecule. Moreover, the distribution of surface charges density for AMTTA molecule was calculated by empirical method. The calculation

was based on Parametric Method (PM3) *ab* initio semi-empirical method with 3-21G* basis set. The fast and accurate Polak-Rieberre algorithm has been used for computation.

3. RESULTS AND DISCUSION

3.1. Inhibitor

The structure of 3-amino-5-methylthio-1H-1,2,4-triazole (AMTTA) molecule is given in Figure 1 which was obtained after a geometric optimization procedure.

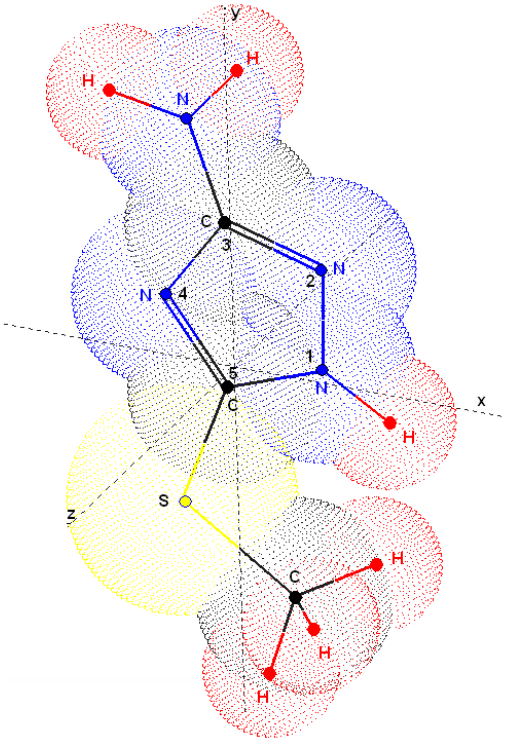

Figure 1. Molecular structure of 3-amino-5-methylthio-1H-1,2,4-triazole (AMTTA) obtained after a geometric optimization procedure using a HyperChem software

The AMTTA compounds is flat molecule, and is stable in air or in majority organic solvents. Moreover, the AMTTA is highly soluble in water. The tested solutions were contained from 0 to 160 mM of 3-amino-5-methylthio-1H-1,2,4-triazole. In acidic medium the AMTTA molecule gives cationic species (with respect to the pK_a = 9.6). The protonated function as shown in the following scheme:

$$AMTTAH + H^+ \leftrightarrow AMTTAH_2^+. \quad (8)$$

Obviously, that in acid solutions the dominant form of inhibitor are the protonated of 3-amino-5-methylthio-1H-1,2,4-triazole molecules. Moreover, other compounds of this type in aqueous acid solutions can exist as protonated cationic species [28-30].

The distribution of surface charges density for AMTTA molecule was calculated by empirical method using HyperChem quantum-mechanical program and listed in Table 1.

Table 1. Element and surface charge density

Element	1 N	2 N	3 C	4 N	5 C	N	S	C
Surface charge density	+0.301	-0.354	-0.048	-0.189	-0.283	+0.143	+0.196	-0.221

It has been found that the largest positive charge (δ^+) is accumulated on the nitrogen (1 N) atom. While the largest negative charge (δ^-) is localized on the nitrogen (2 N) atom (Fig. 1). Therefore, the protonation of AMTT a molecule may be through 2 N atom. Probably, during the electrolysis of $AMTTAH_2^+$ molecules most strongly interact with the surface of the electrode by 2 N atom.

3.2. Potentiodynamic polarization curves

The potentiodynamic measurements were carried out. PD results were given more information about inhibition mechanism corrosion of compounds.

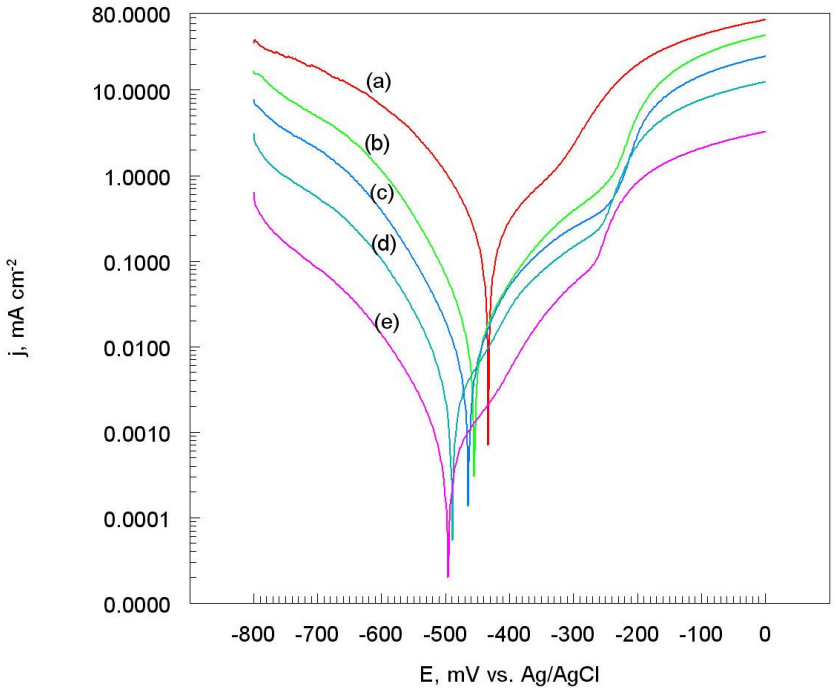

Figure 2. Potentiodynamic polarization curves for C45 mild steel. Solution contained 1.2 M Cl^- and additionally: (a) 0, (b) 40, (c) 80, (d) 120, (e) 160 mM of 3-amino-5-methylthio-1H-1,2,4-triazole, dE/dt 1 mV s^{-1} at 25 ^{0}C

PD measurements were realized in blank test solution and for the presence of various inhibitor concentrations. Figure 2 shows the potentiodynamic polarization curves of C45 mild steel in corrosive solution in the absence and presence of 3-amino-5-methylthio-1H-1,2,4-triazole after 1 hour

immersion. However, curve in Fig. 2 (a) relates to the oxidation of mild steel in solution without of inhibitor. Results showed that, in the area cathodic polarization curves takes place hydrogen evolution mechanism according reactions [26,31]:

$$Fe + H^+ \leftrightarrow (FeH^+)_{ads}, \quad (9)$$

$$(FeH^+)_{ads} + e^- \rightarrow (FeH)_{ads}, \quad (10)$$

$$(FeH)_{ads} + H^+ + e^- \rightarrow Fe + H_2. \quad (11)$$

In anodic polarization, the regular dissolution behavior of C45 mild steel was observed. However, the shorted mechanism of oxidation of iron is as follows:

$$Fe + 2\,H^+ + O_2 \rightarrow (FeO)_{ads} + H_2O - 2\,e^-. \quad (12)$$

Therefore, the electrode was covered with a porous oxide of iron(II) which adhere well to the metal surface. On the other hand for a more positive potential on the electrode of $(FeO)_{ads}$ layer partially was dissolved as a result of the aggressive influence of chloride ions [32]:

$$(FeO)_{ads} + Cl^- + H^+ \leftrightarrow (FeClOH^-)_{ads}, \quad (13)$$

$$(FeClOH^-)_{ads} \leftrightarrow (FeClOH)_{ads} + e^-. \quad (14)$$

The adsorbed layer of hydroxychloride iron(II) in acid solution was dissolved by a simple chemical reaction:

$$(FeClOH)_{ads} + H^+ \leftrightarrow Fe^{2+} + Cl^- + H_2O. \quad (15)$$

Therefore, anodic current density value increased rapidly (Fig. 2, curve (a)).

Consequently, the potentiodynamic polarization curves of C45 mild steel were registered in the solution with various of 3-amino-5-methylthio-1H-1,2,4-triazole concentrations, Figure 2, curves (b) – (e). It can be observed that in the presence of AMTTA, between -800 and 0 mV (vs. Ag/AgCl) current density decreased which is signaled that hydrogen evolution (reactions (9) – (11)) and dissolution of C45 mild steel (reactions (12) – (15)) was reduced. However, increasing the inhibitor concentration decreased dramatically the cathodic and anodic current density values regularly. This was indicative for strongly adhered of 3-amino-5-methylthio-1H-1,2,4-triazole molecules block the surface and prevent anodic dissolution of mild steel. However, the cathodic current – potential diagrams (Fig. 2), which give rise to parallel lines show that increasing concentration of AMTTA do not change the cathodic reduction reaction mechanism of hydrogen ((9) – (11)). The anodic current – potential diagrams show that increasing concentration of AMTTA does alter the mechanism of the anodic dissolution of C45 mild steel. On the basis of potentiodynamic data the corrosion parameters were calculated and the results are summarized in Table 2.

It is clearly seen that the corrosion potential (E_{corr}) values shift to the cathodic region in the presence of 3-amino-5-methylthio-1H-1,2,4-triazole. Due to the displacement in E_{corr} ($\Delta E_{corr} \sim 62$ mV) is lower than 85 mV therefore, the inhibitor can be defined as a mixed type. Consequently, the corrosion current density values decrease almost seventy times for the largest concentration of inhibitor in solution (Table 2). These results indicate that the corrosion current density depends on the AMTTA concentrations. Probably, the AMTTA reduces the corrosion current density values via blocking the active reaction sites on the C45 mild steel surface. Furthermore, determine what processes occur on the electrode surface is very important. This problem will be discussed later in this work.

Table 2. Corrosion parameters and polarization resistance of C45 mild steel in 1.2 M Cl^- for different concentrations of 3-amino-5-methylthio-1H-1,2,4-triazole at 25 ^{0}C

Concentration AMTTA mM	E_{corr} **mV vs. Ag/AgCl**	j_{corr} **mA cm^{-2}**	$-\beta_c$	β_a	**Rp Ω cm^2**
			mV dec^{-1}		
0	-433	0.1800	90	130	2
40	-453	0.0950	100	145	28
80	-463	0.0650	125	165	55
120	-488	0.0300	130	175	136
160	-495	0.0025	135	180	740

The Tafel slopes fit assumes that the process is controlled by the charge transfer and that electrochemical kinetics follow the Butler-Volmer equation. However, the cathodic Tafel slope (β_c) values are generally around expected, considering the hydrogen evolution reaction mechanism on bare steel surface. The anodic Tafel slope (β_a) of linear region provides information about anodic dissolution kinetics during the anodic scan. From potentiodynamic data were determined cathodic or anodic Tafel slopes and are summarized in Table 2. It turned out that both cathodic and anodic Tafel slope values do not change much in the presence of 3-amino-5-methylthio-1H-1,2,4-triazole with respect to blank solution (about 50 mV dec^{-1}). This behavior indicates that the inhibitor merely blocks the corrosion reaction sites of the mild steel and without changes in the mechanism of hydrogen evolution (cathodic) and metal dissolution (anodic) reactions.

The polarization resistance (R_p) values (Eqs. (3) – (5)) are listed in Table 2. It was found that, the R_p values for C45 mild steel electrode increased with an increase of 3-amino-5-methylthio-1H-1,2,4-triazole concentrations. However, the minimum R_p values were 2 and 740 Ω cm^2 in the absence and presence of 160 mM of 3-amino-5-methylthio-1H-1,2,4-triazole respectively. These results indicate that the polarization resistance of electrode depends on the inhibitor concentrations. Therefore, the R_p become dominant in the process of corrosion as a result of the formation of protective layer of AMTTA on C45 mild steel surface. It is clear that the polarization resistance of electrode depends not only on the structure of organic molecules and the nature of the metal but also on the experimental conditions such as concentration of inhibitor and immersion time.

The inhibition efficiency (η) of 3-amino-5-methylthio-1H-1,2,4-triazole was obtained via Eq. (2). The values of η shown in Figure 3. In the presence of inhibitor inhibition efficiency has been steadily increasing, reaching for the largest of AMTT concentration a value of 98%.

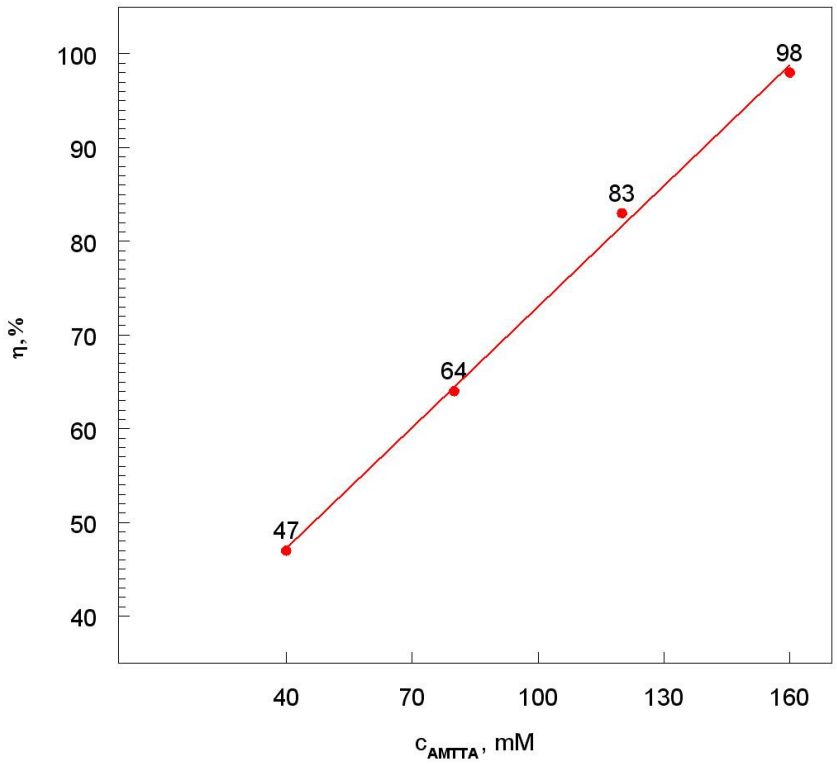

Figure 3. Relation between inhibition efficiency and inhibitor concentrations for C45 mild steel. Solution contained 1.2 M Cl^- and additionally: 40, 80, 120, 160 mM of 3-amino-5-methylthio-1H-1,2,4-triazole at 25 ^{0}C

This detail revels the protective layer of inhibitor molecules may become stronger and thicker attributed to the increasing coverage of compound molecules on metal surface.

3.3. Corrosion rate

The corrosion current density (Table 2) values were converted into the corrosion rate (υ_p) or mass corrosion rate (Δm) (Eqs. (6), (7)) of C45 mild steel in chloride solution in the absence and presence of 3-amino-5-methylthio-1H-1,2,4-triazole. The both corrosion rate values are shown in Figure 4. The corrosion rate and mass corrosion rate of C45 mild steel decreases systematically with increasing of 3-amino-5-methylthio-1H-1,2,4-triazole concentration. The υ_p and Δm values without inhibitor which are about seventy times lower compared to electrolyte with 160 mM of AMTTA.

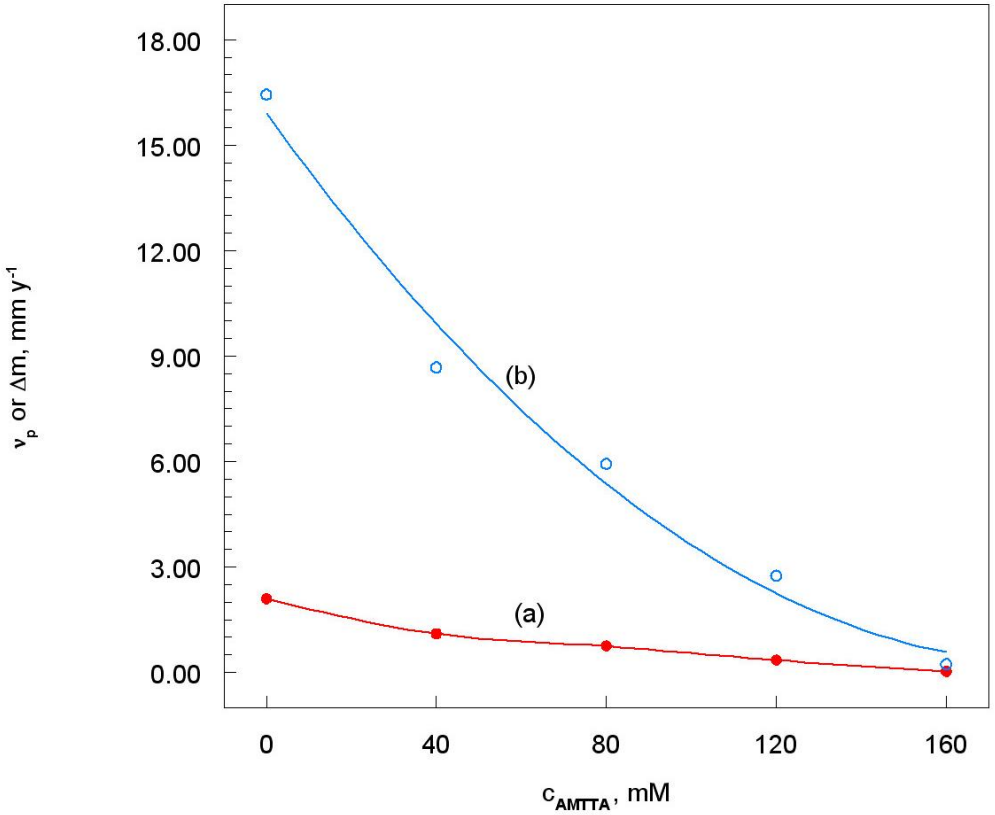

Figure 4. Relationship between: (a) corrosion rate or (b) mass corrosion rate and inhibitor concentrations for C45 mild steel. Solution contained 1.2 M Cl^- and additionally of 3-amino-5-methylthio-1H-1,2,4-triazole at 25 ^{0}C

This result reveals that the inhibitor molecules were adsorbed on the C45 mild steel surface to form the protective layer which protects the metal against corrosion in aggressive chloride environment.

3.4. Chronoamperometric curves

The first step in the action of the inhibitor in corrosive solution is adsorption onto the surface of the metal. The present data shows that 3-amino-5-methylthio-1H-1,2,4-triazole molecules act to decelerate the cathodic or/and anodic reaction corrosion of C45 mild steel. The stability of the adsorbed inhibitor layer was studied by chronoamperometry technique under cathodic and anodic overpotentials for 480 s. The appropriate potential values were selected on the basis of potentiodynamic polarization curves, which were: -700, -200, and -50 mV respectively (vs. Ag/AgCl) (Fig. 2). The chronoamperometric curves recorded for C45 mild steel obtained in 1.2 M Cl^- solution in the presence of 160 mM of 3-amino-5-methylthio-1H-1,2,4-triazole are shown in Figure 5.

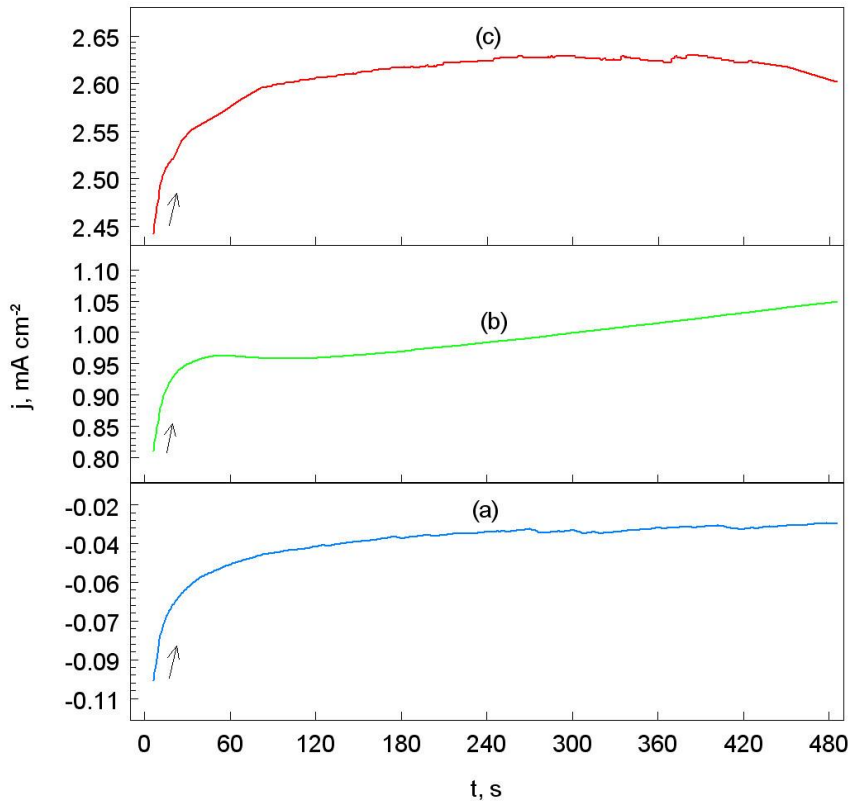

Figure 5. Chronoamperometric curves for C45 mild steel. Solution contained 1.2 M Cl^- and additionally160 mM of 3-amino-5-methylthio-1H-1,2,4-triazole. Potential electrode were: (a) -700, (b) -200, (c) -50 mV at 25 ^{0}C

However, similar curves were obtained for the other concentrations of inhibitor. It was found that in the area of the cathode electrode surface was covered with a layer of 3-amino-5-methylthio-1H-1,2,4-triazole. Therefore, decreasing the cathode current density (which results from the hydrogen evaluation (reactions (9) – (11)) with increasing time of electrolysis (Fig. 5, curve (a)). Is worth noting that in the anodic potential range current density increases systematically (Fig. 5, curve (b)). This means that the inhibitor layer on the C45 mild steel surface is not tight. Furthermore, the process of oxidation of iron (reaction (12)) is only partially inhibited. For the more positive potential of the anodic current density does not change and its value is maintained at a constant level then decreases a slightly (Fig. 5, curve (c)). This case is evident for the stability of protective adsorption layer formed by 3-amino-5-methylthio-1H-1,2,4-triazole on C45 mild steel surface.

3.5. Cyclic polarization curves

The cyclic polarization curves of C45 mild steel in acid chloride solution without and with of various inhibitor concentrations were registered under the same conditions as the potentiodynamic polarization curves (Fig. 2). In this case the cyclic polarization curves are shown as: j = f (t) dependency, Figure 6.

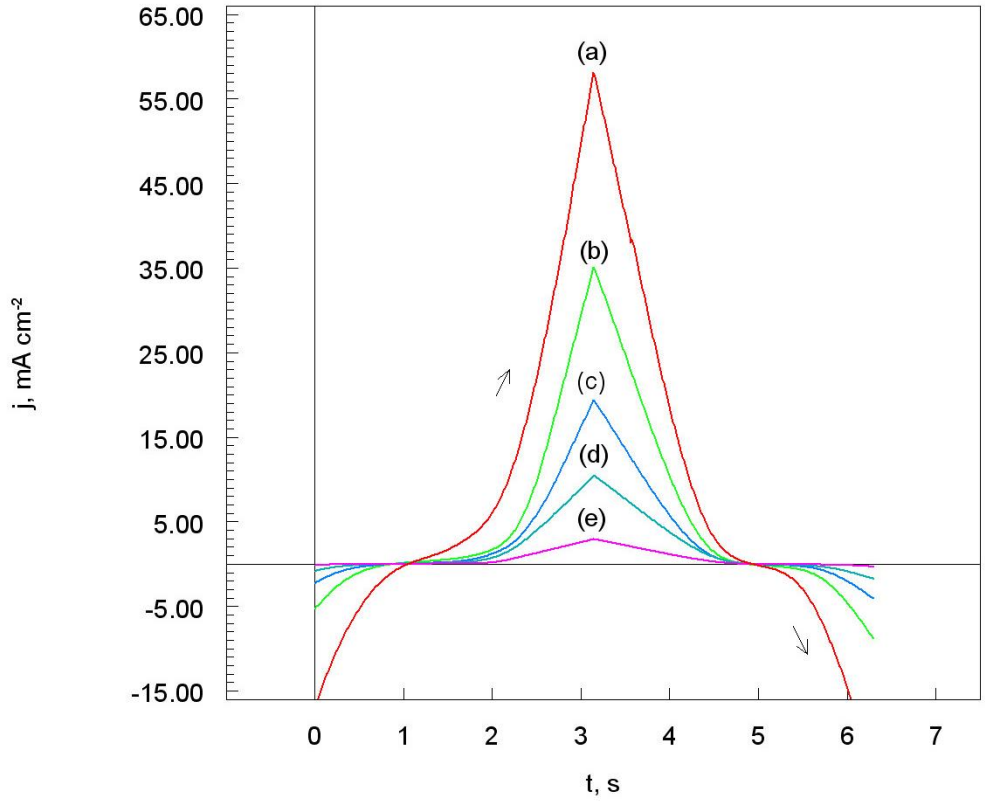

Figure 6. Cyclic polarization curves for C45 mild steel. Solution contained 1.2 M Cl^- and additionally: (a) 0, (b) 40, (c) 80, (d) 120, (e) 160 mM of 3-amino-5-methylthio-1H-1,2,4-triazole, dE/dt 250 mV s^{-1} at 25 ^{0}C

For each test solution the cyclic voltammogram of the second scan was identical to that of first scan. However, the current density corresponding to the oxidation peak of iron decreases gradually with the increasing of 3-amino-5-methylthio-1H-1,2,4-triazole concentrations. Integrating the area under the curves were determined electrical charge consumed by the oxidation of the electrode surface. The values of the electric charges are summarized in Table 3.

Table 3. Electric charge consumed during the oxidation of C45 mild steel surface in 1.2 M Cl^- for different concentrations of 3-amino-5-methylthio-1H-1,2,4-triazole at 25 ^{0}C

Concentration AMTTA (mM)	**0**	**40**	**80**	**120**	**160**
Electric charge (mC)	68.56	38.96	21.82	13.00	4.53

Thus, the experimental results of the present study reveal that the 3-amino-5-methylthio-1H-1,2,4-triazole acts as a corrosion protective layer on C45 mild steel surface in aggressive acid chloride

3.6. Electrochemical impedance spectroscopy

Corrosion behaviour o C45 mild steel specimens in 1.2 M Cl^- solution without and with different concentrations of 3-amino-5-methylthio-1H-1,2,4-triazole was evaluated by electrochemical impedance spectroscopy (EIS) after 1 hour immersion. The Nyquist plots of mild steel in acid chloride solutions in the absence and presence of inhibitor are shown in Figure 7.

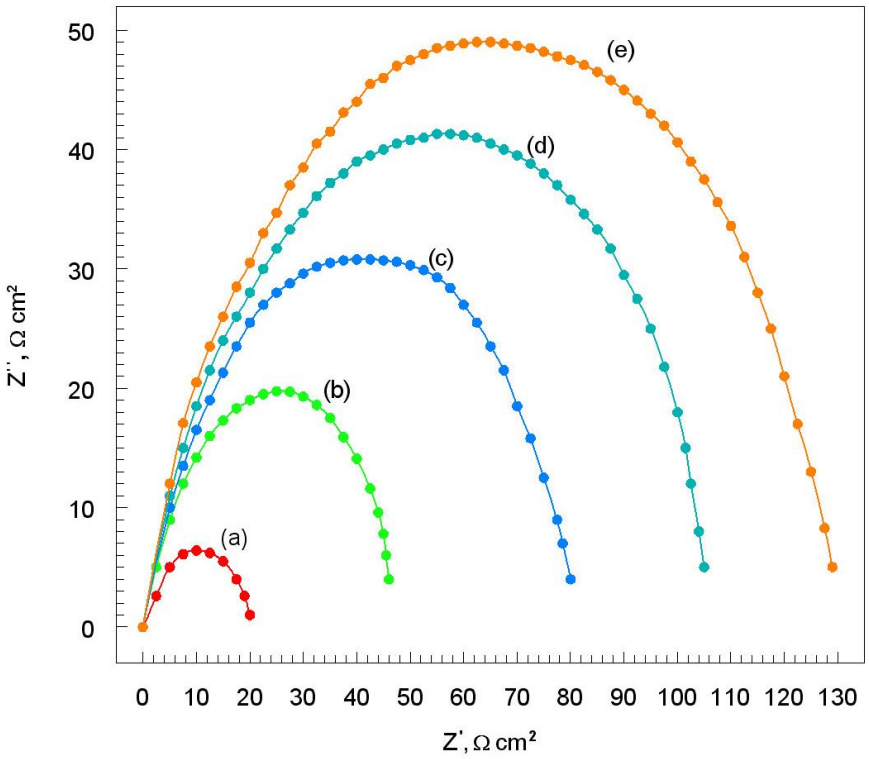

Figure 7. Nyquist plots for C45 mild steel. Solution contained 1.2 M Cl^- and additionally: (a) 0, (b) 40, (c) 80, (d) 120, (e) 160 mM of 3-amino-5-methylthio-1H-1,2,4-triazole at 25 ^{0}C

The depressed semicircles in impedance spectra indicate a non-ideal electrochemical behaviour at the solid/liquid interface. Nyquist plot for uninhibited solution (curve (a)) shows a small inductive behaviour at low frequencies. Moreover, the addition of 3-amino-5-methylthio-1H-1,2,4-triazole (curves (b) – (e)) does not change the type of the shape, therefore compound control the activity of the corrosion reaction rather than inflect its nature. Is evident from Fig. 7 the diameters of the capacitive loop in the inhibited solution is greater than that in the blank solution (curve (a)) which suggests the corrosion process is restrained by AMTTA. As a result protective adsorption layer formed on mild steel surface exhibit as an effective barrier property to the corrosive media. The presence of low frequency inductive loop in presence of AMTTA may be attributed to the relaxation process obtained by adsorption of species like $(Cl^-)_{ads}$ and $(H^+)_{ads}$ on the electrode surface.

Bode plots as the absolute impedance and phase angle vs. frequency for C45 mild steel in acid chloride solutions with and without of 3-amino-5-methylthio-1H-1,2,4-triazole are presented in Figures 8a and 8b.

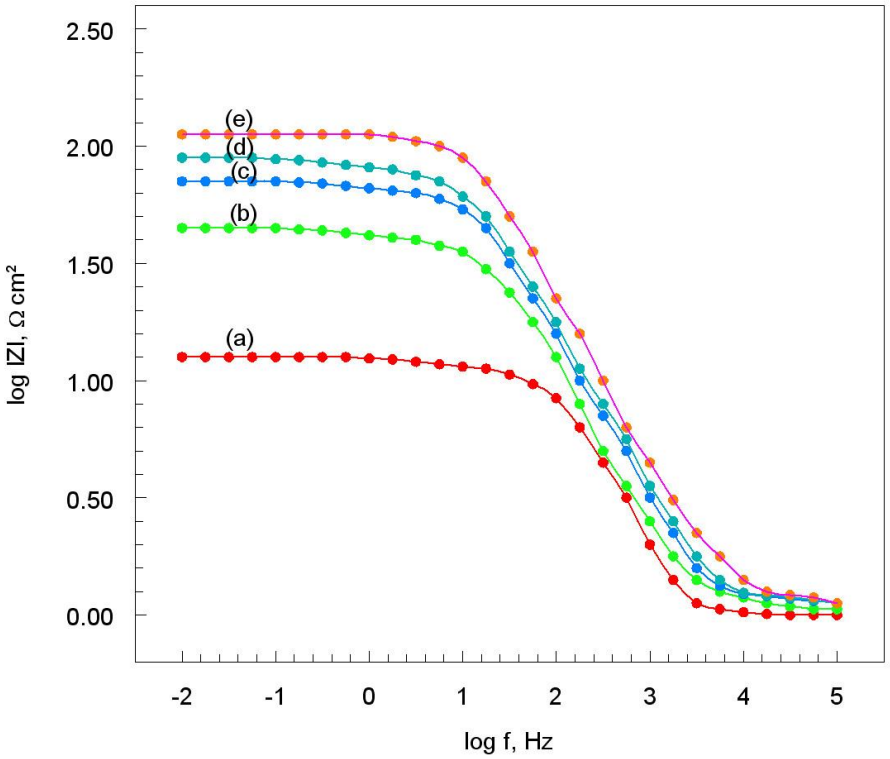

Figure 8a. Absolute impedance plots for C45 mild steel. Solution contained 1.2 M Cl^- and additionally: (a) 0, (b) 40, (c) 80, (d) 120, (e) 160 mM of 3-amino-5-methylthio-1H-1,2,4-triazole at 25 ^{0}C

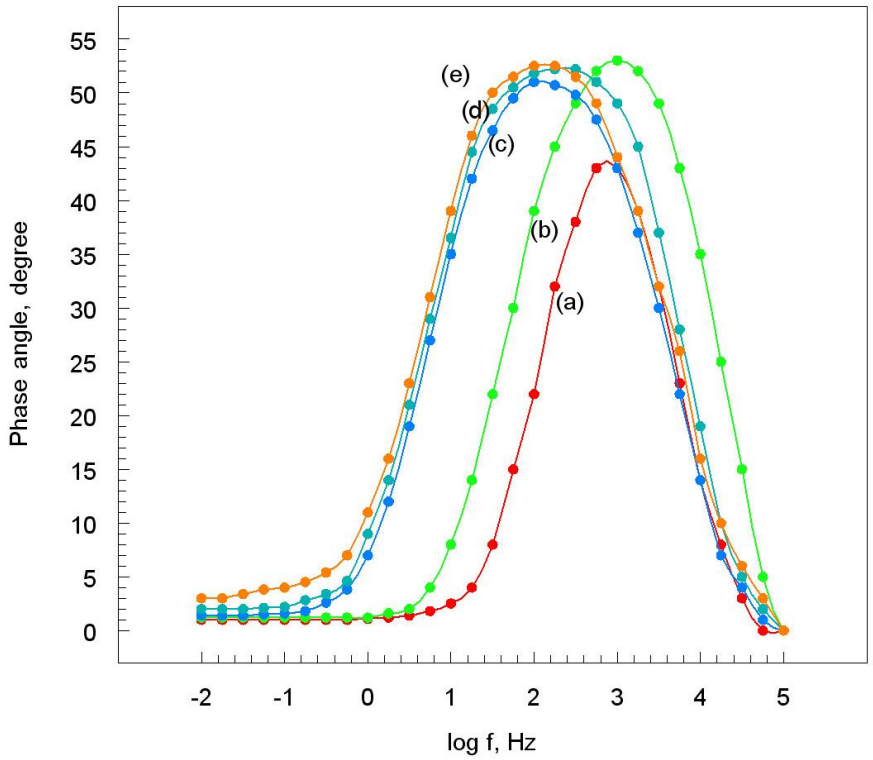

Figure 8b. Phase angle plots for C45 mild steel. Solution contained 1.2 M Cl^- and additionally: (a) 0, (b) 40, (c) 80, (d) 120, (e) 160 mM of 3-amino-5-methylthio-1H-1,2,4-triazole at 25 ^{0}C

Inhibition ability of AMTTA can be observed from impedance values at the low frequency and the increasing absolute impedance value indicates the higher inhibition efficiency of 3-amino-5-methylthio-1H-1,2,4-triazole (Fig. 8a). Moreover, according to shifting trend of phase angle plots raising the concentration of AMTTA conduces to more negative values of the phase angle which indicates the better inhibitive behaviour of 3-amino-5-methylthio-1H-1,2,4-triazole with higher concentration. Figure 8b) shows only a phase peaks in the studied frequency range, suggesting the sole time constant connected with the formation of double layer capacitance at solid/liquid interface.

Electrical equivalent circuits are generally used to model the electrochemical behavior and to calculate the impedance parameters. Based on the measurement results the impedance data was fitted via the equivalent circuit as *RL*(*QR*) model which is presented in Figure 9.

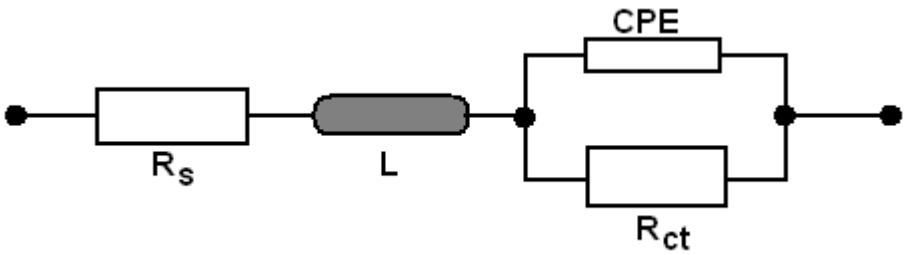

Figure 9. Electrochemical equivalent circuit for fitting EIS data (*RL*(*QR*)), R_s is the solution resistance, L is the inductance, CPE is the constant phase element, R_{ct} is the charge transfer resistance

The corroding surface of C45 mild steel in 1.2 M Cl^- is expected to be inhomogeneous because of its roughness therefore, the capacitance is presented through a constant phase element (CPE). The impedance element of the CPE is represented by the equation [30]:

$$Z_{CPE} = Y_0^{-1} (j\,\omega)^{-n}, \quad (16)$$

where Y_0 is the proportional factor (CPE constant), $j^2 = -1$ is the imaginary number, ω is the angular frequency, and n is the deviation parameter (CPE exponent) when ($-1 \leq n \leq 1$) means a phase shift depending on its whole number value (for $n = 0$, CPE represents a pure resistance).

The double layer capacitance and inhibition efficiency were calculated as the following formulae:

$$C_{dl} = Y_0 \left(j\,\omega_m^n\right)^{n-1}, \quad (17)$$

and:

$$\eta = \frac{R_{ct} - R_{ct}^0}{R_{ct}} \times 100\,, \quad (18)$$

where $\omega^n{}_m$ is the angular frequency, R_{ct} and $R^0{}_{ct}$ are charge transfer resistance values in the presence and absence inhibitor, respectively. The values of C_{dl} are expressed by the Helmholtz model.

The impedance data obtained from the equivalent circuit are listed in Table 4. However, EIS results are more reliable (in compare to potentiodynamic measurements) because the measurements were done close to the corrosion potential and it consider as non-destructive test due to small magnitude of the applied potential (i.e. 10 mV). This small perturbation of the corrosion potential

minimizes surface modification and errors associated with large deviations from the electrochemical equilibrium.

Table 4. Electrochemical impedance results and inhibition efficiency for C45 mild steel in 1.2 M Cl^- for different concentrations of 3-amino-5-methylthio-1H-1,2,4-triazole at 25 ^{0}C

Concentration AMTTA mM	R_s **Ω cm^2**	R_{ct} **Ω cm^2**	C_{dl} **µF cm^{-2}**	L **µH cm^2**	η **%**
0	0.26	13.9	769	0.48	---
40	0.41	26.2	649	0.39	47
80	0.69	40.2	497	0.32	65
120	0.96	89.1	430	0.26	84
160	1.60	326.2	171	0.29	96

The results of Table 4 show the R_s values increase with increasing of 3-amino-5-methylthio-1H-1,2,4-triazole concentrations, because the inhibitor reduces the conductivity of the electrolytes. The R_{ct} values increase with increasing inhibitor concentrations because the adsorbed layer of inhibitor impedes the exchange of electric charge between the electrode surface and the electrolyte. However, the trend is opposite for C_{dl}. The decrease in C_{dl} suggests a fading in the local dielectric constant or an enhancement in the thickness of the capacitor attributed to the adsorption of more AMTTA molecules on the C45 mild steel surface. The inductance (L) decreases slightly with increasing concentration of inhibitor (Table 4). Moreover, the inhibition efficiency of 3-amino-5-methylthio-1H-1,2,4-triazole values are similar to the η values which were obtained from the potentiodynamic polarization curves (Fig. 3).

3.7. Adsorption isotherm

The adsorption behavior of inhibitor molecule on metal surface can be assessed by several adsorption isotherms [33]. In order to obtain the adsorption isotherm surface coverage degree (Θ) as function of inhibitor concentration was calculated based on the corrosion current density values according to equation:

$$\Theta = \frac{j_{corr}^0 - j_{corr}}{j_{corr}^0}, \quad (19)$$

Moreover, the surface coverage degree can be calculated by using the formula:

$$\Theta = \frac{Q^0 - Q_{inh}}{Q^0}, \quad (19a)$$

where Q^0 and Q_{inh} were the charges in the absence and presence of the inhibitor, respectively in the test solution.

The surface coverage degree of C45 mild steel in 1.2 M Cl^- for different concentrations of 3-amino-5-methylthio-1H-1,2,4-triazole which were calculated based on the equations (19) and (19a) are listed in Table 5. However, the average value of the inhibition efficiency was about 95%.

Table 5. Surface coverage degree of C45 mild steel in 1.2 M Cl^- for different concentrations of 3-amino-5-methylthio-1H-1,2,4-triazole at 25 ^{0}C

Concentration AMTTA (mM)	**40**	**80**	**120**	**160**
Surface coverage degree (equation (19))	0.47	0.64	0.83	0.98
Surface coverage degree (equation (19a))	0.43	0.68	0.81	0.93
Average values	0.45	0.66	0.82	0.95

Attempts were made to fit the average values of Θ to various isotherms and the best fit was obtained using the Temkin adsorption isotherm which can be described by the following equation [34]:

$$\log\left(\frac{\Theta}{c_{AMTTA}}\right) = \log K_{ads} - g\Theta, \quad (20)$$

where g is the adsorbate interaction parameter, and K_{ads} is the adsorptive equilibrium constant, which can be obtained from the intercept of straight line on the log (Θ / c_{AMTTA}) versus Θ plot. Moreover, the standard free energy of adsorption (ΔG^0_{ads}) can be estimated by the following equation [26,35]:

$$\Delta G^0_{ads} = -RT\ln(55.5 K_{ads}), \quad (21)$$

where the value of 55.5 is the molar concentration of water in solution, R is the molar gas constant, and T is the absolute temperature.

Figure 10 shows the Temkin adsorption plot for C45 mild steel in 1.2 M Cl^- solution containing different concentrations of 3-amino-5-methylthio-1H-1,2,4-triazole. The adsorption parameters are completed in Table 6. The Temkin isotherm showed a good correlation with experimental data. The negative slope g = -0.55 indicates the existence of a repulsive lateral interaction of inhibitor molecules in the adsorption layer. Moreover, the value of K_{ads} was calculated to be 19.6 M^{-1}.

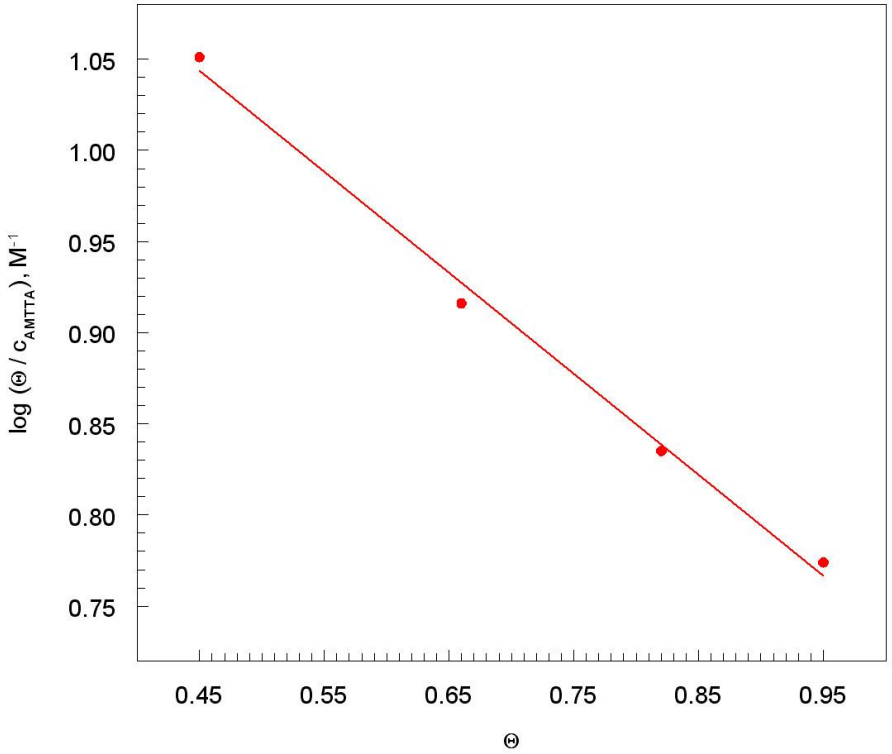

Figure 10. Temkin adsorption plot for C45 mild steel. Solution contained 1.2 M Cl^- and additionally of 3-amino-5-methylthio-1H-1,2,4-triazole at 25 ^{0}C

A low value of the adsorptive equilibrium constant indicates a weak interaction of AMTT molecules with of C45 mild steel surface.

Table 6. Adsorption parameters for 3-amino-5-methylthio-1H-1,2,4-triazole on C45 mild steel surface in 1.2 M Cl^- at 25 ^{0}C

Inhibitor	R^2	g	K_{ads} M^{-1}	ΔG^0_{ads} kJ mol^{-1}
AMTTA	0.9971	-0.55	19.6	-17.32

Moreover, the value of ΔG^0_{ads} was found to be -17.32 kJ mol^{-1}. In the case of this study the calculated of standard free energy of adsorption value is small (Table 6) which means that the adsorption of AMTTA on C45 mild steel surface in 1.2 M Cl^- solution is a typical physisorption [36].

The primary step in the action of organic corrosion inhibitors in acid solutions is usually adsorption at the metal – solution interface. Physisorption is due to electrostatic attractive forces between inhibiting organic ions or dipoles and the electrically charged surface of the metal. However, this problem will be discussed in the further part of the article.

In Table 7 were listed literature data with regarded to inhibition efficiency, equilibrium constant adsorption, standard free energy of adsorption of 1,2,4-triazole derivatives for mild steel in different corrosion environments.

Table 7. Type of inhibitor, concentration, environment, inhibition efficiency, equilibrium constant adsorption, standard free energy of adsorption, and reference

Inhibitor	**Concentration**	**Environment**	***η*** **%**	K_{ads} **M^{-1}**	ΔG^0_{ads} **kJ mol^{-1}**	**Reference**
1.	160 mM	1 M NaCl and 0.2 M HCl, (1.2 M Cl^-)	95	19.6	-17.32	Authors
2.	0.1 mM	0.5 M H_2SO_4	99.2	8.9×10^4	-38.2	[37]
3.	0.4 mM	1 M HCl	96.8	2.2×10^5	-40.76	[38]
4.1. 4.2. 4.3.	0.4 mM	2.5 M H_2SO_4	99.1 98.3 94.7	8.6×10^5 2.5×10^5 4.5×10^4	-42.45 -41.18 -37.05	[39]
5.1. 5.2. 5.3.	200 ppm	1M HCl	94.76 95.49 96.28	---	---	[40]
6.1 6.2 6.3	150 mg/ L	1 M HCl	95 89 85	3.4×10^4 1.5×10^4 8.5×10^4	-37.0 -35.0 -33.4	[41]
7.1. 7.2. 7.3.	0.05 g/ L	0,5 M HCl	85.02 86.90 94.20	11.325 28.375 35.714	-16.2 -18.6 -19.1	[42]
8.1. 8.2.	1 mM	2 M H_3PO_4	85.72 83.49	1.66×10^5 1.00×10^5	-41.07 -39.77	[43]

1. 3-amino-5-methylthio-1H-1,2,4-triazole
2. 4,4-dimethyl-3oxo-2-(1,2,4)triazol-1-yl-pentanethioic acid phenylamide
3. 2,5-bis(4-methoxyphenyl)-4-amino-1,2,4-triazole

4.1. 4-amino-5-phenyl-4H-1,2,4-triazole-3-thiol
4.2. 4-amino-5-methyl-4H-1,2,4-triazole-3-thiol
4.3. 4-amino-3-hydrazino-5-mercapto-1,2,4-trazole,4-amino-5-hydrazine-1,2,4-triazole-3-thiol

5. 1. 4-amino-4H-1,2,4-triazole-3,5-dimethanol

5.2. (4-(benzyliddeneamino)-4H-1,2,4-triazole-3,5-diyl)dimethanol
5.3. (4-(4-(dimethylamino)benzylideneamino))-4H-1,2,4-triazole-3,5-diyl)dimethanol
6.1. (3-phenylallylidene)amino-5-(pyridine-4-yl)-4H-1,2,4-triazole-3-thiol
6.2. 3-mercapto-5(pyridine-4-yl-4H-1,2,4-triazole-4-yl)imino)methyl)phenol
6.3. (4-nitrobenzylidene)amino)-5-(pyridine-4-yl)-4H-1,2,4-triazole-3-thiol
7.1. 8-bromo-5-morpholino-3-(4-propylphenyl)-[1,2,4] triazolo[4,3-c]pyrimidine
7.2. 8-bromo-3-(2-fluoro-3-methoxyphenyl)-5-morpholino-[1,2,4]triazolo[4,3-c]pyrimidine
7.3. 8-bromo-3-(2-fluoro-4,5-dimethoxy-phenyl)-5-morpholin-4-yl-[1,2,4]triazolo[4,3-c]pyrimidine
8.1. 3,5-bis(4-methoxyphenyl)-4-amino-1,2,4-triazole
8.2. 3,5-bis(4-chlorophenyl)-4-amino-1,2,4-triazole

The results of the study (Table 7) show that all 1,2,4-triazole derivatives excellent inhibit the corrosion process of mild steel in aggressive environments. The adsorption of 1,2,4-triazole derivatives on mild steel surface obeyed Langmuir adsorption model. This isotherm assumed that the adsorbed molecules occupied only one site and there were no interaction with other adsorbed molecules. In the case of 3-amino-5-methylthio-1H-1,2,4-triazole (which we have studied) appears lateral interaction of inhibitor molecules in the layer of adsorption, which it creates in result of physical adsorption. However, the ΔG^0_{ads} values were informed that the adsorption mechanism of 1,2,4-triazole derivatives on the mild steel surface in aggressive solutions were typical of chemisorption (with the exception of inhibitor labeled as 7). The negative values of ΔG^0_{ads} ensure the spontaneity of the adsorption process of inhibitors and stability of the adsorbed layer on the steels surface.

3.8. Inverted metallographic microscope studies

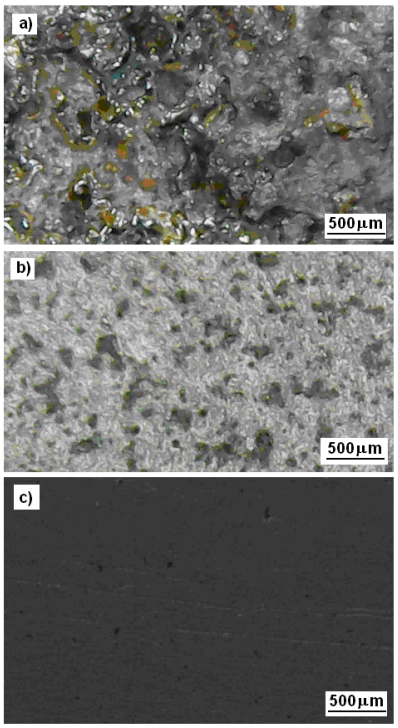

Figure 11. Inverted metallographic microscope images of C45 mild steel: a) after treated in 1.2 M Cl^- solution, b) after treated in 1.2 M Cl^- solution in presence 160 mM of 3-amino-5-methylthio-1H-1,2,4-triazole, c) after the removal of protective layer. Exposure time of 240 hours at 25 ^{0}C

The surface studies of C45 mild steel specimens were analyzed by inverted metallographic microscope (IMM) after 240 hours immersion time in the absence (1.2 M Cl^-) and presence of 160 mM of 3-amino-5-methylthio-1H-1,2,4-triazole, Figure 11.

It can be clearly seen from Figure 11a) that the steel surface was strongly damaged in the absence of inhibitor due to metal dissolution in acidic media. Furthermore, the C45 mild steel surface has porous structure and many cracks with large deep holes. The IMM image of mild steel in the presence of AMTTA (Fig. 11b)) has very different appearance after 240 hours immersion time. As a result of physical adsorption the specimen surface was covered with a layer of inhibitor. However, the inhibitor adsorbed layer on the steel surface provides a protective barrier which isolates the access of aggressive chloride solution to the steel surface. Figure 11c) shows the surface of the steel after the removal (by 1 M HCl solution) of protective layer. Can see clearly that the 3-amino-5-methylthio-1H-1,2,4-triazole reduced metal dissolution remarkably and the surface is highly smooth and free from cracks or cavitations. Thus it can be concluded that the surface coverage was good and adsorption layer is highly protective.

3.9. Mechanism of inhibition

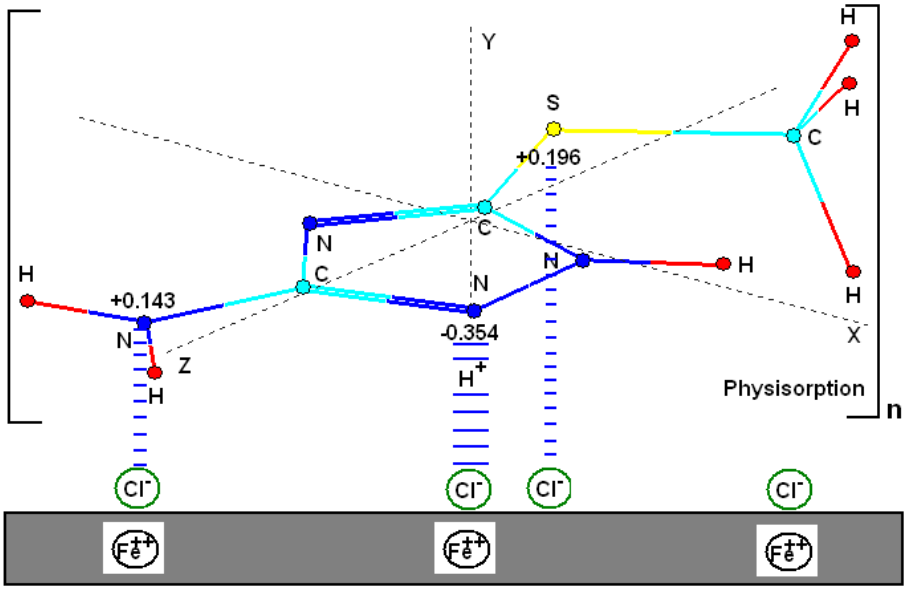

Figure 12. Proposal of models of protective layer on C45 mild steel surface in presence of 3-amino-5-methylthio-1H-1,2,4-triazole in acid chloride solution

The corrosion inhibition mechanism in acid medium the most often depends on the adsorption of an inhibitor onto the metal surface. Moreover, organic inhibitor possess inhibiting ability by the formation of protective film on the metal surface and the adsorption behaviour is mainly determined by the electrostatic interaction between the metal and the inhibitor. Obtained results helped to propose a model of protective layer which may be formed on C45 mild steel surface in presence of 3-amino-5-

methylthio-1H-1,2,4-triazole in acid chloride solution. In this case the interaction between adsorbed inhibitor and metal surface can be defined as electrostatic interaction between the charged of $AMTTAH^{+}_{2}$ (reaction (8)) and electrode surface (physisorption). Due to the acquired results of experiments and theoretical calculation a credible inference of the adsorption process is expressed by Figure 12. It seems that Cl- ions (reactions (13) and (14)) are first adsorbed on the metal surface and the net positive charge on the mild steel surface enhances the specific adsorption of chloride ions [44].

As a result of electrostatic interaction the protonated of $AMTTAH^{+}_{2}$ molecules are attracted toward the Cl^{-} ions. On the other hand the positively charged nitrogen (from $-NH_2$ group) and sulfur atoms in addition an electrostatically interact with Cl^{-} ions which are chemisorbed on C45 mild steel surface (Fig. 12).

Probably in this way was created a protective film on metal surface which effectively protected the mild steel surface against the corrosive effects of aggressive environment.

4. CONCLUSION

The 3-amino-5-methylthio-1H-1,2,4-triazole (AMTTA) have been studied as corrosion inhibitor for mild steel in acid chloride solution. The main conclusions are as follows:

1. The adsorption of 3-amino-5-methylthio-1H-1,2,4-triazole onto the C45 mild steel surface was characterized by the decrease in: cathodic and anodic current densities observed in the potentiodynamic polarization curves and the double-layer capacitance computed from electrochemical impedance spectroscopy experiments.

2. The AMTTA act as good inhibitor for the corrosion of mild steel in acid chloride (1.2 M Cl^{-}) solution. The 3-amino-5-methylthio-1H-1,2,4-triazole compound behaves as mixed type corrosion inhibitor by inhibiting both cathodic hydrogen evolution and anodic metal dissolution reactions.

3. The corrosion inhibition efficiencies of mild steel were increased with increasing of 3-amino-5-methylthio-1H-1,2,4-triazole concentrations. Good agreement between the inhibition efficiencies calculated using different techniques was obtained. It was found that the average inhibition efficiency was about 95%.

4. The corrosion rate and mass corrosion rate of investigated of C45 mild steel were decreased with increasing of 3-amino-5-methylthio-1H-1,2,4-triazole concentrations.

5. The best fit to the experimental data was Temkin adsorption isotherm. The standard free energy of adsorption (ΔG^{0}_{ads}) value was found to be -17.32 kJ mol^{-1}. Moreover, it was shown that the adsorption of AMTTA on the C45 mild steel surface takes place through physical adsorption.

6. Inverted metallographic microscope images indicated a very good protective film on the C45 mild steel surface after 240 hours immersion in the presence of 160 mM AMTTA in 1.2 M Cl^{-}. The AMTTA molecule acts by blocking the mild steel surface.

7. The quantum chemical study shows that the possible physical adsorption center of the inhibitor is nitrogen atom (2 N) of the 3-amino-5-methylthio-1H-1,2,4-triazole.

References

1. N.A. Negm, M.F. Zaki, M.M. Said, S.M. Morsy, *Corros. Sci*., 53 (2011) 4233.
2. J.J. Fu, H.S. Zang, Y. Wang, S.N. Li, T. Chen, X.D. Liu, *Ind. Eng. Chem. Res.*, 51 (2012) 6377.
3. D. Daoud, T. Douadi, S. Issaadi, S. Chafaa, *Corros. Sci.,* 79 (2014) 50.
4. S.A. El-Masksoud, *Appl. Surf. Sci*., 206 (2003) 129.
5. M. Lebrini, F. Bentiss, H. Vezin, M. Lagrene´e, *Corros. Sci.*, 48 (2006) 1279.
6. T. Touhami, A. Aounti, Y. Abed, B. Hammouti, S. Kertit, A. Ramdani, K. Elkacemi, *Corros. Sci*., 42 (2000) 929.
7. A.S. Algaber, E.M. El-Nemna, M.M. Saleh, *Mater. Chem. Phys*., 86 (2004) 26.
8. M.A. Quairshi, R. Sardar, D. Jamel, *Mater. Chem. Phys*., 71 (2001) 309.
9. E.E. Oguzie, G.N. Onuoha, A.I. Onuchukwu, *Mater. Chem. Phys*., 89 (2005) 305.
10. L. Larabi, Y. Harek, M. Traisnel, A. Mansri, *J. Appl. Electrochem.*, 34 (2004) 833.
11. K.F. Khaled, *Mater. Chem. Phys.,* 125 (2011) 427.
12. E.M. Sherif, *Mater. Chem. Phys.,* 129 (2011) 961.
13. M.P. Desimone, G. Grundemeier, G. Gordillo, S.N. Simson, *Electrochim. Acta,* 56 (2011) 2990.
14. M.A.J. Mazumder, H.A. El-Muallem, M. Faiz, S.A. Ali, *Corros. Sci.*, 87 (2014) 187.
15. L. Feng, H. Yang, F. Wang, *Electrochim. Acta,* 58 (2011) 427.
16. N. Dkhireche, A. Dahami, A. Rochdi, J. Hmimou, R. Touir, M. Eban Touhami, M. El-Bakri, A. El-Hallaoui, A. Anouar, H. Takenouti, *J. Ind. Eng. Chem.*, 19 (2013) 1996.
17. F. Bentiss, M. Traisnel, H. Vezin, M. Lagrene'e, *Corros. Sci.*, 45 (2003) 371.
18. S. Tramilselvi, S. Rajeswari, *Anti-Corros. Meth. Mater*., 50 (2003) 223.
19. H.-L. Wang, R.-B. Liu, J. Xin, *Corros. Sci.*, 46 (2004) 2455.
20. E.H. El-Ashry, A. El Nemr, S.A. Esawy, S. Ragab, *Electrochim. Acta,* 51 (2006) 3957.
21. F. Bentiss, M. Bounasis, B. Mernari, M. Traisnel, H. Vezin, M. Lagrene'e, *Appl. Surf. Sci.*, 253 (2007) 3696.
22. M. Lebrini, M. Traisnel, M. Lagrene'e, B. Mernari, F. Bentiss, *Corros. Sci*., 50 (2008) 473.
23. S. Zhang, Z. Tao, S. Liao, F. Wu, *Corros. Sci*., 52 (2010) 3126.
24. E.M. Sherif, S.-M. Park, *Electrochim. Acta,* 51 (2006) 1313.
25. S.A. Abd El-Maksoud, H.H. Hassan, *Mater. Corros*., 58 (2007) 369.
26. M. Scendo, J. Trela, K. Staszewska, *Int. J. Electrochem. Sci.,* 11 (2016) 2666.
27. M. Scendo, N. Radek, J. Konstanty, K. Staszewska, *Arch. Metall. Mater*., 61 (2016) 1895.
28. A.R. Katritzky, Comprehensive Heterocyclic Chemistry, *The Structure, Reaction, Synthesis and Uses of Heterocyclic Compounds*, 5, Pergamon Press Ltd., London, 1984.
29. M. Scendo, *Corros. Sci*., 49 (2007) 2985.
30. B.D. Mert, A.O. Yüce, G. Kardas, B. Yazici, *Corros. Sci*., 85 (2014) 287.
31. M. Scendo, J. Trela, N. Radek, *Corros. Rev*., 30 (2012) 33.
32. R.J. Chin, K. Nobe, *J. Electrochem. Soc.*, 119 (1972) 1457.
33. S.P. Cardoso, F.A. Reis, F.C. Massapust, J.F. Costa, L.S. Tebaldi, L.F.L. Araujo, M.V.A. Silva, T.S. Oliveira, J.A.C.P. Gomes, E. Hollauer, *Quim. Nova,* 28 (2005) 756.
34. F.S. de Souza, A. Spinelli, *Corros. Sci*., 51 (2009) 642.
35. A. Ehsani, H. Mohammad Shiri, M.G. Mahjani, R. Moshrefi, R. Safari, *Kovove Mater*., 54 (2016) 233.
36. X. Zhou, H. Yang, F. Wang, *Corros. Sci*., 54 (2012) 193.
37. Z. Tao, S. Zhang, W. Li, B. Hou, *Corros. Sci.*, 51 (2009) 2588.
38. F. Bentiss, Ch. Jama, B. Mernari, H. El-Attari, L. El-Kadi, M. Lebrini, M. Traisnel, M. Lagrene'e, *Corros. Sci.*, 51 (2009) 1628.
39. A.Y. Musa, A.A.H. Kadhum, A.B. Mohamad. M.S. Takriff, *Corros. Sci.,* 52 (2010) 3331.
40. S. John, A. Joseph, *Mater. Chem. Phys.,* 133 (2012) 1083.
41. K.R. Ansari, M.A. Quraishi, A. Singh, *Corros. Sci.*, 79 (2014) 5.

42. D.M. Gurudatt, K.N. Mohana, H.C. Tandon, *J. Mol. Liquids*, 211 (2015) 275.
43. M. El-Belghiti, Y. Karzazi, A. Dafali, B. Hammouti, F. Bentiss, L.B. Obot, I. Bahadur, E.E. Ebenso, *J. Mol. Liquids*, 218 (2016) 281.
44. M. Lagrene'e, B. Mernari, M. Bouanis, M. Traisnel, F. Bentiss, *Corros. Sci.*, 44 (2002) 573.